MYU Tokyo

S & M 3535

Photoluminescence, Scintillation, and Thermally Stimulated Luminescence Properties of Eu-doped Al_2O_3 Single Crystals

Ren Tsubouchi,[1] Hiroyuki Fukushima,[1] Takumi Kato,[2] Daisuke Nakauchi,[2] Satoshi Saijo,[1] Toru Matsuura,[1] Noriaki Kawaguchi,[2] Tomoaki Yoneda,[1] and Takayuki Yanagida[2*]

[1]Department of Electrical and Electronic Engineering, National Institute of Technology, Fukui College, Geshi, Sabae, Fukui 916-8507, Japan
[2]Division of Materials Science, Nara Institute of Science and Technology, 8916-5 Takayama-cho, Ikoma, Nara 630-0192, Japan

(Received October 31, 2023; accepted January 22, 2024)

Keywords: photoluminescence, scintillation, TSL, single crystal, floating zone

The photoluminescence (PL), scintillation, and thermally stimulated luminescence (TSL) properties of Eu-doped (0.01, 0.1, and 1%) Al_2O_3 single crystals grown by the floating zone method were investigated systematically. The PL of the samples showed several sharp emission peaks across 550–750 nm originating from the 4f–4f transitions of Eu^{3+} and the 3d–3d transitions of Cr^{3+} impurity ions. The scintillation spectrum of the samples showed a broad emission peak at 320 nm due to the F^+ center and an emission peak at 700 nm due to the 3d–3d transitions of Cr^{3+} impurity ions. All the samples showed TSL glow peaks at around 200, 320, and 375 °C. The TSL intensity of the 1% Eu-doped sample was the highest among the present three samples, and the TSL response was proportional to the irradiated X-ray dose in the range from 10 to 1000 mGy. The Eu-doped Al_2O_3 single crystal could be a novel candidate for personal dose monitoring applications.

1. Introduction

Radiation-induced phosphors can be classified into two types: scintillators, in which carriers are excited by ionizing radiation irradiation at the luminescent center and immediately emit light, and phosphor-based dosimeters, in which captured carriers are re-excited by external stimulation such as heat or light, leading to emission.(1,2) Scintillators are applied in medical imaging equipment such as X-ray computed tomography (CT) and positron emission tomography (PET), security equipment such as baggage screening devices, and environmental monitoring.(1,3,4) In contrast, phosphor-based dosimeters are mainly applied in personal dose monitoring.(5–7) The luminescence types of phosphor-based dosimeters are classified as follows: thermally stimulated luminescence (TSL), in which carriers are re-excited by thermal stimulation; optically stimulated luminescence (OSL), in which carriers are re-excited by light;

*Corresponding author: e-mail: t-yanagida@ms.naist.jp
https://doi.org/10.18494/SAM4763

ISSN 0914-4935 © MYU K.K.
https://myukk.org/

and radio-photoluminescence (RPL), in which the interaction with ionizing radiation creates new emission centers in the material.(8–12)

So far, LiF single crystals doped with Ti and Mg(13) and Cu-doped LiB_4O_7 ceramics(14) for TSL, BeO ceramics(15) for OSL, and Ag-doped phosphate glass(16,17) for RPL have been studied. In particular, personal dosimeters should have an effective atomic number (Z_{eff}) close to that of human soft tissue (Z_{eff} = 7.51) from the viewpoint of bioequivalence, in addition to high sensitivity dose–response characteristics and low fading.(18) To develop novel phosphor-based dosimeters, the TSL, OSL, and RPL properties of many new materials have been investigated.(19–29) In particular, Al_2O_3 has high thermal stability, chemical stability, and low Z_{eff}; thus, C-doped Al_2O_3 is commercially developed as TSL and OSL personal dosimeters.(7,30)

In recent years, transparent ceramics, which have more defects than single crystals, have been attracting attention in phosphor-based dosimeter applications.(31–34) Moreover, the TSL and OSL properties of Al_2O_3 transparent ceramics doped with C, Mg, Ti, Ce, and Eu have also been studied.(35–38) In contrast, there are few reports on Al_2O_3 single crystals doped with impurities other than C, leaving room for further research.

Single crystals are expected to have a higher detection efficiency than opaque ceramics because of their high transmittance and the ease of extracting internally generated light to the outside. In addition, the mass production of large-area transparent ceramics is difficult with current technology. In contrast, single crystals are suitable for mass production because large-area single crystals can be fabricated by the pulling method such as the Czochralski method. Therefore, if dosimeters that emit light with high efficiency in single-crystal form are discovered, they could be one of the best candidates for new dosimeter materials compared with opaque and transparent ceramics. Recently, $MgAl_2O_4$ and Mg_2SiO_4 single crystals doped with some dopants have been studied as candidates for new dosimeter materials, realizing defects produced in single-crystal form with high transmittance and high TSL and OSL intensities.(39–44) In this study, Eu^{3+} is selected as a luminescence center. Eu^{3+} ions are often used as luminescence centers because they have intense red emission due to the 4f–4f transition.(45) To date, the PL, scintillation, and TSL properties of Eu-doped Al_2O_3 transparent ceramics have been reported.(38,46) In Al_2O_3, it is considered necessary to evaluate dosimetric properties not only in the transparent ceramic form but also in the single-crystal form. For the above reasons, Eu-doped Al_2O_3 single crystals exhibit intense luminescence and good TSL properties.

In this study, Eu-doped Al_2O_3 single crystals were synthesized by the floating zone (FZ) method, and in addition to their PL and scintillation properties, their TSL response properties as a dosimeter were also investigated.

2. Materials and Methods

Eu-doped Al_2O_3 single crystals were synthesized using an FZ furnace equipped with four xenon lamps. Al_2O_3 (99.99%) and Eu_2O_3 (99.99%) were used as starting materials and were mixed uniformly using a mortar and pestle. The nominal doped concentrations of Eu were 0.01, 0.1, and 1%. The X-ray powder diffraction (XRD) patterns were measured in the range of 20–80° (Rigaku, UltimaIV). The PL emission was measured using a CCD-based spectrometer

(Otsuka Electronics, MCPD-9800-2285C). The excitation source was a xenon lamp with a monochromator, and the excitation light was led to the sample through an optical fiber. The X-ray-induced scintillation spectra were measured using laboratory-made setups.(47) The applied voltage and tube current during the measurement of scintillation spectra were 40 kV and 1.2 mA, respectively. The TSL glow curves were measured using a TSL reader (TL-2000, Nanogray) after X-ray irradiation. No background processing was conducted for the blackbody radiation signal.

3. Results and Discussion

Figure 1 shows a photograph of the Eu-doped Al_2O_3 single crystals. The samples were approximately 1 mm thick and colorless. The following measurements were conducted using these samples. The actual Eu concentration inside the crystal was considered to be lower than the nominal concentration. The weights of the 0.01, 0.1, and 1% Eu-doped Al_2O_3 single crystals were 0.0592, 0.0211, and 0.0204 g, respectively.

Figure 2 shows the XRD patterns of the Eu-doped Al_2O_3 single crystals. The remaining crushed samples were used for XRD measurements. The XRD patterns of the samples matched the reference pattern for Al_2O_3 (ICSD. No. 31545). Therefore, the samples are considered to be single-phase Al_2O_3. The coincidence of the valence and coordination numbers of Al^{3+} and Eu^{3+} suggested that Eu^{3+} ions were substituted at the Al^{3+} site.

Figure 3 shows the PL excitation and emission spectra of the Eu-doped Al_2O_3 single crystals. The Eu-doped samples showed emission peaks at 587, 616, 678, and 714 nm. These emission peaks are consistent with those attributed to the 4f–4f transition of Eu^{3+}.(38,48,49) The sharp emission peak at 693 nm is considered to be due to the 3d–3d transition of Cr^{3+}.(37,46) The intensity of the emission peak due to the 4f–4f transition of Eu^{3+} weakened as the Eu doping concentration increased. This is the same trend reported previously for Eu-doped Al_2O_3

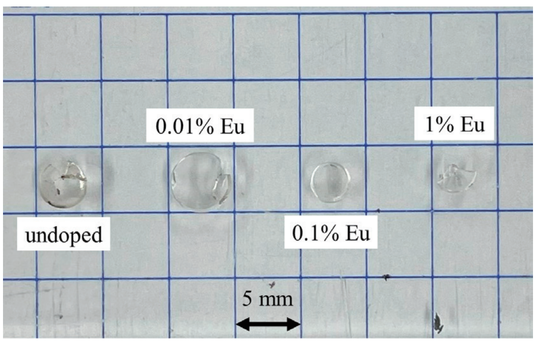

Fig. 1. (Color online) Photograph of Eu-doped Al_2O_3 single crystals.

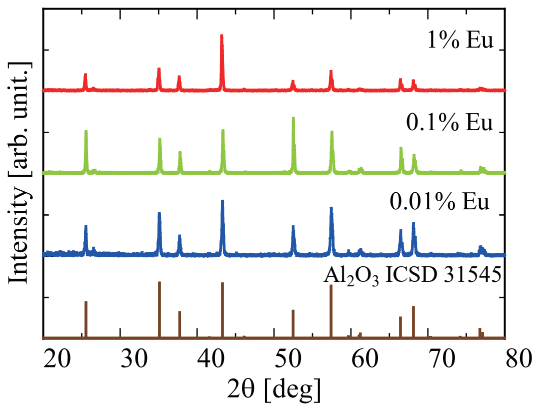

Fig. 2. (Color online) XRD patterns of Eu-doped Al_2O_3 single crystals.

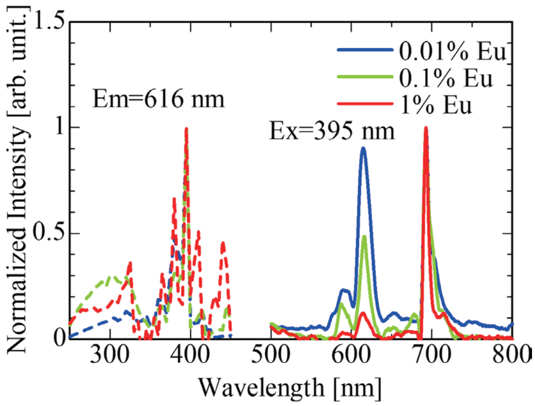

Fig. 3. (Color online) PL emission and excitation spectra of Eu-doped Al_2O_3 single crystals.

transparent ceramics. Since the samples in this study were synthesized in air ambient, emission peaks originating from the 4f–4f transition of Eu^{3+} were observed while no emission bands originating from the 5d–4f transition of Eu^{2+} were observed. Excitation spectra showed sharp peaks at 365, 380, 395, and 415 nm. These peaks are attributed to the 4f–4f transition of Eu^{3+}.(38,48,49) The broad peak at about 300 nm is attributed to charge transfer transitions between Eu^{3+} and O^{2-}.

Figure 4 shows X-ray-induced scintillation spectra of Eu-doped Al_2O_3 single crystals. A broad scintillation peak was observed at ~320 nm. On the basis of previous studies, the scintillation peak at 320 nm is attributed to the F+ center.(35,46,50) As with PL, the emission near 700 nm is considered to be a peak due to the 3d–3d transition of Cr^{3+}. No emission due to the 4f–4f transition of Eu^{3+}, which was observed in the PL spectra, was observed. PL directly excites carriers to the luminescent center, and recombination leads to luminescence. In scintillation, carriers are ionized, transferred to the luminescent center via energy transport, and recombined to emit light. The luminescence mechanism differs between PL and scintillation, and in scintillation, the carriers do not always recombine at the desired emission center. Therefore, in Eu-doped Al_2O_3 single crystals, the luminescence was attributed to Cr^{3+} rather than Eu^{3+} ions.

Figure 5 shows the TSL glow curves of Eu-doped Al_2O_3 single crystals after 1000 mGy X-ray irradiation. The TSL intensity was normalized by sample weight. All the samples showed TSL glow peaks at ~200, ~320, and ~375 °C. The 1% Eu-doped sample showed the highest TSL intensity among the present samples. Since the ionic radius of Eu^{3+} (0.947 Å, 6-coordination) is larger than that of Al^{3+} (0.535 Å, 6-coordination), strain is generated, and defects are formed when Eu^{3+} ions are substituted at the Al^{3+} sites. Therefore, 1% Eu-doped Al_2O_3 single crystals have the strongest TSL intensity because the generated number of defects is greater than those of the other samples. Figure 6 shows the fitted curves of the TSL glow curve of the 1% Eu-doped Al_2O_3 single crystal. The TSL glow curve was fitted with a general order kinetics in the formula shown below.(51) The obtained parameters are listed in Table 1. The 1% Eu-doped sample showed peaks at 150, 187, 221, 320, and 380 °C. The shapes of the TSL glow curves between Eu-doped Al_2O_3 single crystals and those in transparent ceramics are different. In a previous study, Eu-

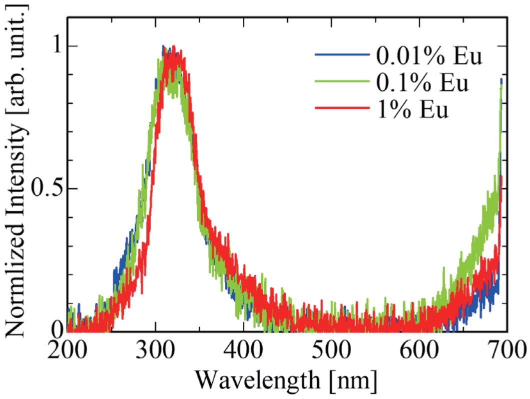

Fig. 4. (Color online) X-ray-induced scintillation spectra of Eu-doped Al_2O_3 single crystals.

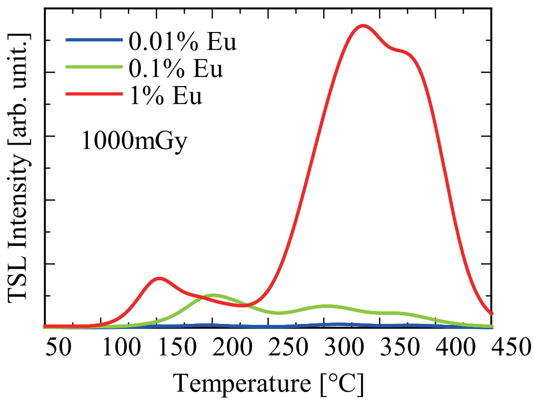

Fig. 5. (Color online) TSL glow curves of Eu-doped Al_2O_3 single crystals.

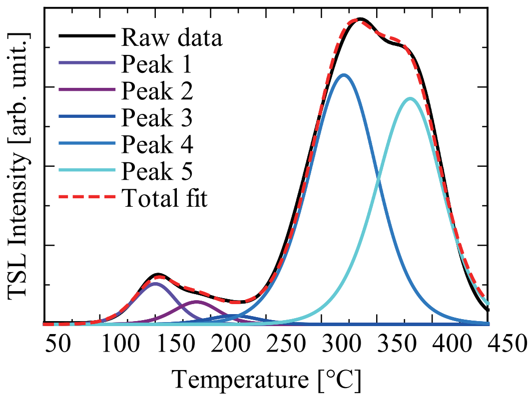

Fig. 6. (Color online) Fitted curves of TSL glow curve of 1% Eu-doped Al_2O_3 single crystal.

Table 1
Parameters of fitted glow curves using 1% Eu-doped Al_2O_3 single crystal.

		Peak intensity (arb. unit)	Peak temperature (°C)	Trap depth (eV)	Frequency factor (s^{-1})
	Peak 1	33	150	1.02	1.48×10^{11}
	Peak 2	18	187	1.11	1.38×10^{11}
1% Eu	Peak 3	7	221	1.14	3.66×10^{10}
	Peak 4	201	320	1.21	1.21×10^{9}
	Peak 5	182	380	1.51	2.93×10^{10}

doped Al_2O_3 transparent ceramics showed the TSL glow peak at ~100 °C.[46] In contrast, the present Eu-doped Al_2O_3 single crystals showed no TSL glow peak at ~100 °C. The defects generated depend on the fabrication method. Typically, single crystals have fewer defects than transparent ceramics.

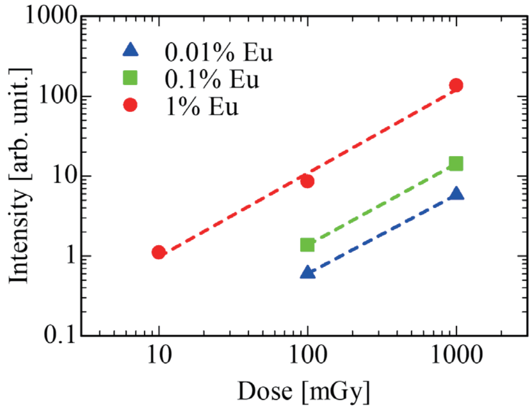

Fig. 7. (Color online) TSL dose response functions of Eu-doped Al_2O_3 single crystals.

$$I(T)=I_M b^{\frac{b}{b-1}} \exp\left(\frac{E}{kT}\frac{T-T_M}{T_M}\right)\left[1+(b-1)\frac{2kT_M}{E}+(b-1)\left(1-\frac{2kT}{E}\right)\left(\frac{T^2}{T_M^2}\exp\left(\frac{E}{kT}\frac{T-T_M}{T_M}\right)\right)\right]^{\frac{-b}{b-1}} \quad (1)$$

Figure 7 shows the TSL dose response functions of Eu-doped Al_2O_3 single crystals. The TSL intensity at each dose represents the maximum intensity at 300 °C. The TSL intensity increased linearly with irradiation dose in the range of 10–1000 mGy for the 1% Eu-doped sample and in the range of 100–1000 mGy for the 0.01 and 0.1% Eu-doped samples. In the previous study of Eu-doped Al_2O_3 transparent ceramics, the TSL intensity decreased with increasing Eu doping concentration.(46) In contrast, Eu-doped Al_2O_3 single crystals showed a trend toward higher TSL intensity with increasing Eu doping concentration. The number of defects may increase with increasing Eu doping concentration, and the TSL intensity depends on the number of defects. Thus, the highly Eu-doped Al_2O_3 single crystals exhibited strong TSL intensity. The lower sensitivity limit of the Eu-doped Al_2O_3 single crystal was 10 mGy, which is higher than the detection limit of 10–100 μGy in the personal dose monitoring application. In future works, we would like to improve the TSL intensity by growing Al_2O_3 doped with different luminescent centers and annealing in a reducing atmosphere.

4. Conclusions

Eu-doped (0.01, 0.1, and 1%) Al_2O_3 single crystals were successfully grown by the FZ method. In terms of PL, the samples showed several sharp emission peaks across 550–750 nm originating from the 4f–4f transitions of Eu^{3+}. In terms of scintillation, the samples showed a broad emission peak at 320 nm due to the F^+ center. Furthermore, the Eu-doped Al_2O_3 single crystals showed PL and scintillation due to not only Eu^{3+} but also Cr^{3+} impurity ions. In terms of TSL, all the samples showed TSL glow peaks at ~200, 320, and 375 °C, and the TSL intensity of the 1% Eu-doped sample was the highest among the present samples. The absence of the TSL peak at ~100 °C is suggested to be advantageous for applications such as personal dose monitoring. The TSL response was confirmed to be linearly related to the irradiated X-ray dose in the range from 10 to 1000 mGy. Therefore, the Eu-doped Al_2O_3 single crystal can be a novel candidate for personal dose monitoring applications.

Acknowledgments

This work was supported by Grants-in-Aid for Scientific Research A (22H00309), Scientific Research B (22H03872, 22H02939, 21H03733, and 21H03736), Early-Career Scientists (23K13689), and Challenging Exploratory Research (22K18997) from the Japan Society for the Promotion of Science. The Cooperative Research Project of the Research Center for Biomedical Engineering, A-STEP (JPMJTM22DN) from JST, Kazuchika Okura Memorial Foundation, Asahi Glass Foundation, Nakatani Foundation, and Konica Minolta Science and Technology Foundation are also acknowledged.

References

1 T. Yanagida: Proc. Jpn. Acad. Ser. B **94** (2018) 75. https://doi.org/10.2183/pjab.94.007
2 T. Yanagida, T. Kato, D. Nakauchi, and N. Kawaguchi: Jpn. J. Appl. Phys. **62** (2023) 010508. https://doi.org/10.35848/1347-4065/ac9026
3 D. Totsuka, T. Yanagida, K. Fukuda, N. Kawaguchi, Y. Fujimoto, J. Pejchal, Y. Yokota, and A. Yoshikawa: Nucl. Instrum. Methods Phys. Res., Sect. A **659** (2011) 399. https://doi.org/10.1016/j.nima.2011.08.014
4 J. Azorin Nieto: Appl. Radiat. Isot. **117** (2016) 135. https://doi.org/10.1016/j.apradiso.2015.11.111
5 M. Iwao, H. Takase, D. Shiratori, D. Nakauchi, T. Kato, N. Kawaguchi, and T. Yanagida: Radiat. Meas. **140** (2021) 106492. https://doi.org/10.1016/j.radmeas.2020.106492
6 Y. Miyamoto, Y. Takei, H. Nanto, T. Kurobori, A. Konnai, T. Yanagida, A. Yoshikawa, Y. Shimotsuma, M. Sakakura, K. Miura, K. Hirao, Y. Nagashima, and T. Yamamoto: Radiat. Meas. **46** (2011) 1480. https://doi.org/10.1016/j.radmeas.2011.05.048
7 S. W. S. McKeever, M. S. Akselrod, and B. G. Markey: Radiat. Prot. Dosim. **65** (1996) 267. https://doi.org/10.1093/oxfordjournals.rpd.a031639
8 T. Yanagida: J. Lumin. **169** (2016) 544. https://doi.org/10.1016/j.jlumin.2015.01.006
9 T. Kato, D. Nakauchi, N. Kawaguchi, and T. Yanagida: Mater. Lett. **270** (2020) 127688. https://doi.org/10.1016/j.matlet.2020.127688
10 T. Yanagida, G. Okada, T. Kato, D. Nakauchi, and N. Kawaguchi: Radiat. Meas. **158** (2022) 106847. https://doi.org/10.1016/j.radmeas.2022.106847
11 H. Nanto and G. Okada: Jpn. J. Appl. Phys. **62** (2023) 010505. https://doi.org/10.35848/1347-4065/ac9106
12 G. Okada, Y. Koguchi, T. Yanagida, S. Kasap, and H. Nanto: Jpn. J. Appl. Phys. **62** (2023) 010609. https://doi.org/10.35848/1347-4065/ac9023
13 A. Lushchik, I. Kudryavtseva, P. Liblik, Ch. Lushchik, A. I. Nepomnyashchikh, K. Schwartz, and E. Vasil‘chenko: Radiat. Meas. **43** (2008) 157. https://doi.org/10.1016/j.radmeas.2007.10.001
14 G. Kitis, G. S. Polymeris, I. K. Sfampa, M. Prokic, N. Meriç, and V. Pagonis: Radiat. Meas. **84** (2016) 15. https://doi.org/10.1016/j.radmeas.2015.11.002
15 E. Bulur and H. Y. Göksu: Radiat. Meas. **29** (1998) 639. https://doi.org/10.1016/S1350-4487(98)00084-5
16 Y. Miyamoto, Y. Takei, H. Nanto, T. Kurobori, A. Konnai, T. Yanagida, A. Yoshikawa, Y. Shimotsuma, M. Sakakura, K. Miura, K. Hirao, Y. Nagashima, and T. Yamamoto: Radiat. Meas. **46** (2011) 1480. https://doi.org/10.1016/j.radmeas.2011.05.048
17 H. Kawamoto, M. Koshimizu, Y. Fujimoto, and K. Asai: Jpn. J. Appl. Phys. **62** (2023) 010501. https://doi.org/10.35848/1347-4065/ac9cb0
18 T. Kato, N. Kawano, G. Okada, N. Kawaguchi, and T. Yanagida: Radiat. Meas. **107** (2017) 43. https://doi.org/10.1016/j.radmeas.2017.09.006
19 Y. Takebuchi, T. Kato, D. Nakauchi, N. Kawaguchi, and T. Yanagida: Sens. Mater. **34** (2022) 645. https://doi.org/10.18494/SAM3685
20 D. Shiratori, Y. Takebuchi, T. Kato, D. Nakauchi, N. Kawaguchi, and T. Yanagida: Sens. Mater. **34** (2022) 745. https://doi.org/10.18494/SAM3695

21 T. Kato, D. Nakauchi, N. Kawaguchi, and T. Yanagida: Sens. Mater. **34** (2022) 653. https://doi.org/10.18494/SAM3682
22 T. Kato, D. Shiratori, M. Iwao, H. Takase, D. Nakauchi, N. Kawaguchi, and T. Yanagida: Sens. Mater. **33** (2021) 2163. https://doi.org/10.18494/SAM.2021.3318
23 H. Kimura, T. Kato, D. Nakauchi, N. Kawaguchi, and T. Yanagida: Sens. Mater. **33** (2021) 2187. https://doi.org/10.18494/SAM.2021.3322
24 D. Shiratori, T. Kato, D. Nakauchi, N. Kawaguchi, and T. Yanagida: Sens. Mater. **33** (2021) 2171. https://doi.org/10.18494/SAM.2021.3317
25 T. Kato, H. Kimura, K. Okazaki, D. Nakauchi, N. Kawaguchi, and T. Yanagida: Sens. Mater. **35** (2023) 483. https://doi.org/10.18494/SAM4137
26 T. Kato, D. Nakauchi, N. Kawaguchi, and T. Yanagida: Sens. Mater **34** (2022) 653. https://doi.org/10.18494/SAM3682
27 K. Ichiba, Y. Takebuchi, H. Kimura, D. Shiratori, T. Kato, D. Nakauchi, N. Kawaguchi, and T. Yanagida: Sens. Mater. **34** (2022) 677. https://doi.org/10.18494/SAM3680
28 G. Ito, H. Kimura, D. Shiratori, D. Nakauchi, T. Kato, N. Kawaguchi, and T. Yanagida: Sens. Mater. **34** (2022) 685. https://doi.org/10.18494/SAM3681
29 H. Nanto, G. Okada, K. Hirasawa, Y. Koguchi, W. Shinozaki, S. Ueno, Y. Yanagida, F. d'Errico, and T. Yamamoto: Sens. Mater. **34** (2022) 757. https://doi.org/10.18494/SAM3686
30 S. W. S. McKeever: Radiat. Meas. **46** (2011) 1336. https://doi.org/10.1016/j.radmeas.2011.02.016
31 T. Kato, G. Okada, and T. Yanagida: Ceram. Int. **42** (2016) 5617. https://doi.org/10.1016/j.ceramint.2015.12.070
32 F. Nakamura, T. Kato, G. Okada, N. Kawaguchi, K. Fukuda, and T. Yanagida: Ceram. Int. **43** (2017) 7211. https://doi.org/10.1016/j.ceramint.2017.03.009
33 T. Kato, D. Nakauchi, N. Kawaguchi, and T. Yanagida: Jpn. J. Appl. Phys. **62** (2023) 010604. https://doi.org/10.35848/1347-4065/ac94ff
34 H. Kimura, T. Kato, T. Fujiwara, M. Tanaka, D. Nakauchi, N. Kawaguchi, and T. Yanagida: Jpn. J. Appl. Phys. **62** (2023) 010504. https://doi.org/10.35848/1347-4065/ac916c
35 T. Kato, N. Kawano, G. Okada, N. Kawaguchi, and T. Yanagida: Nucl. Instrum. Methods Phys. Res., Sect. B **435** (2018) 296. https://doi.org/10.1016/j.nimb.2017.12.013
36 Q. Liu, Q. Yang, G. Zhao, and S. Lu: J. Alloys Compd. **582** (2014) 754. https://doi.org/10.1016/j.jallcom.2013.07.189
37 T. Kato, H. Fukushima, D. Nakauchi, N. Kawaguchi, and T. Yanagida: Optik **264** (2022) 169435. https://doi.org/10.1016/j.ijleo.2022.169435
38 R. Klement, K. Drdlíková, M. Kachlík, D. Drdlík, D. Galusek, and K. Maca: J. Eur. Ceram. Soc. **41** (2021) 4896. https://doi.org/10.1016/j.jeurceramsoc.2021.03.029
39 Y. Takebuchi, H. Fukushima, T. Kato, D. Nakauchi, N. Kawaguchi, and T. Yanagida: Radiat. Phys. Chem. **177** (2020) 109163. https://doi.org/10.1016/j.radphyschem.2020.109163
40 Y. Takebuchi, M. Koshimizu, T. Kato, D. Nakauchi, N. Kawaguchi, and T. Yanagida: J. Lumin. **251** (2022) 119247. https://doi.org/10.1016/j.jlumin.2022.119247
41 Y. Takebuchi, H. Fukushima, D. Nakauchi, T. Kato, N. Kawaguchi, and T. Yanagida: J. Lumin. **223** (2020) 117139. https://doi.org/10.1016/j.jlumin.2020.117139
42 Y. Takebuchi, H. Fukushima, T. Kato, D. Nakauchi, N. Kawaguchi, and T. Yanagida: Optik **231** (2021) 166498. https://doi.org/10.1016/j.ijleo.2021.166498
43 K. Ichiba, Y. Takebuchi, H. Kimura, T. Kato, D. Nakauchi, N. Kawaguchi, and T. Yanagida: Sens. Mater. **35** (2023) 475. https://doi.org/10.18494/SAM4143
44 G. Okada, T. Kojima, J. Ushizawa, N. Kawaguchi, and T. Yanagida: Curr. Appl. Phys. **17** (2017) 422. https://doi.org/10.1016/j.cap.2017.01.004
45 N. Kawano, G. Okada, H. Kimura, and T. Yanagida: Ceram. Int. **46** (2020) 26339. https://doi.org/10.1016/j.ceramint.2020.06.092
46 N. Kawano, T. Kato, G. Okada, N. Kawaguchi, and T. Yanagida: Opt. Mater. **88** (2019) 67. https://doi.org/10.1016/j.optmat.2018.11.002
47 T. Yanagida, K. Kamada, Y. Fujimoto, H. Yagi, and T. Yanagitani: Opt. Mater. **35** (2013) 2480. https://doi.org/10.1016/j.optmat.2013.07.002
48 J. H. Hong, J. Y. Lee, J. H. Kang, J. Y. Lee, H. S. Jang, S.-Y. Cho, and D. H. Kim: Ceram. Int. **48** (2022) 32886. https://doi.org/10.1016/j.ceramint.2022.07.216
49 D. Liu and Z. Zhu: J. Alloys Compd. **583** (2014) 291. https://doi.org/10.1016/j.jallcom.2013.08.173
50 B. D. Evans and M. Stapelbroek: Phys. Rev. B: Condens. Matter **18** (1978) 7089. https://doi.org/10.1103/PhysRevB.18.7089
51 G. Kitis, J. M. Gomez-Ros, and J. W. N. Tuyn: J. Phys. D: Appl. Phys. **31** (1998) 2636. https://doi.org/10.1088/0022-3727/31/19/037